


Estimation of stature from femur length measured using computed tomography after the analysis of three-dimensional characteristics of femur bone in Korean cadavers

Sookyoung Lee¹ · Ho-hyeon Gong² · Jin-young Hyun³ · Hyung-nam Koo² · Han-young Lee² · Nak-eun Chung⁴ · Young-shik Choi¹ · Kyung-moo Yang¹ · Byung Ha Choi¹ 

Received: 29 August 2016 / Accepted: 3 February 2017 / Published online: 20 February 2017
© Springer-Verlag Berlin Heidelberg 2017

Abstract Estimation of stature is a basic and important forensic procedure in identifying decomposed or skeletonized bodies. Due to advances in radiologic equipment, forensic science frequently uses computed tomography (CT) and software to apply these findings to investigations. Technical developments have increased the accuracy of the measurement of various bones. However, there are still some inaccuracies, such as defining correct landmarks in three-dimensional (3D) images. Femur length is frequently used for calculation of stature, but because it is a 3D structure, the digital image may not always correlate with the femur length measured with an osteometric board. However, more studies are now showing that the maximum femur length calculated in 3D imagery is comparable to the maximum femur length calculated using an osteometric board. This study used digitalized data of the femur obtained from the CT image through the specialized software. The digitalized femur images were put on the virtual osteometric board, which helped us to understand the anatomic characteristics of the femur and to confirm that the maximum femur lengths calculated in 3D images are similar to the results obtained using an osteometric board. These data were used to obtain a stature estimation formula for the Korean population.

Keywords Estimation of stature · Femur length · Three-dimensional images · Osteometric board

Introduction

Estimation of stature in severely decomposed or skeletonized bodies is one of the most important aspects in the forensic field [1–3]. The femur is usually the best choice for stature estimation, although bones such as the tibia, humerus, ulna, radius, scapula, cranium, sternum, sacrum, and the bones of the hand and foot are also used for measurement [4–9]. However, the long bones are most commonly used because there is a proportional correlation between stature and long bones [10].

The use of radiologic tools in routine autopsy can yield additional information such as serious radiologic findings and important measurements [11]. Multiple reports have suggested the usefulness of three-dimensional (3D) computed tomography (CT) images in anthropology [12, 13]. Previous studies have shown that measurements collected using multi-detector computed tomography (MDCT) have the potential risk of technical error due to uncertainty in landmark location [14]. Validating the accuracy of the data obtained by radiologic measurements must be done before using the data in routine work.

Recent advances in 3D image processing software have improved the understanding of 3D structures and increased the possibility of accurate measurements [15]. Digital Imaging and Communications in Medicine (DICOM) files can be converted into computer-assisted design (CAD) data using the software Materialise's Interactive Medical Image Control System (MIMICS) (Materialise NV, Leuven, Belgium). In this software, all the landmarks have specific coordinates, which makes it possible to measure all the lengths and all the angles easily.

✉ Byung Ha Choi
pathosky51@gmail.com

¹ Medical Examiner's Office, National Forensic Service, 139, Jiyang-ro, Yangcheon-gu, Seoul 08036, South Korea

² Department of Forensic Investigation, National Forensic Service, 139, Jiyang-ro, Yangcheon-gu, Seoul 08036, South Korea

³ Department of Forensic Medicine, National Forensic Service, 1524, Yuseong-daero, Yuseong-gu, Daejeon 34054, South Korea

⁴ Medical Examiner's Office, National Forensic Service, 10, Ipchun-ro, Wonju-si, Gangwon-do 26460, South Korea

When using measurement data from MDCT, a problem is that femur lengths measured using digital images may not be the same as the lengths measured with the osteometric board, because the femur is a 3D structure. As seen in Fig. 1a, the distance between the two vertical planes (L1) may not be the same as the maximum femur length measured using CT (L2) [12]. If, however, the two lines are parallel to each other, then the lengths should be the same, which would render the digital data acceptable to use for anthropologic purposes.

It is believed that the proportional correlations between stature and long bones vary among the different population and generation [16–18]. Choi et al. developed a stature estimation formula for Korean adult males that is somewhat different from other stature estimation formulae [19]. No data have yet been reported concerning stature estimation for Korean females.

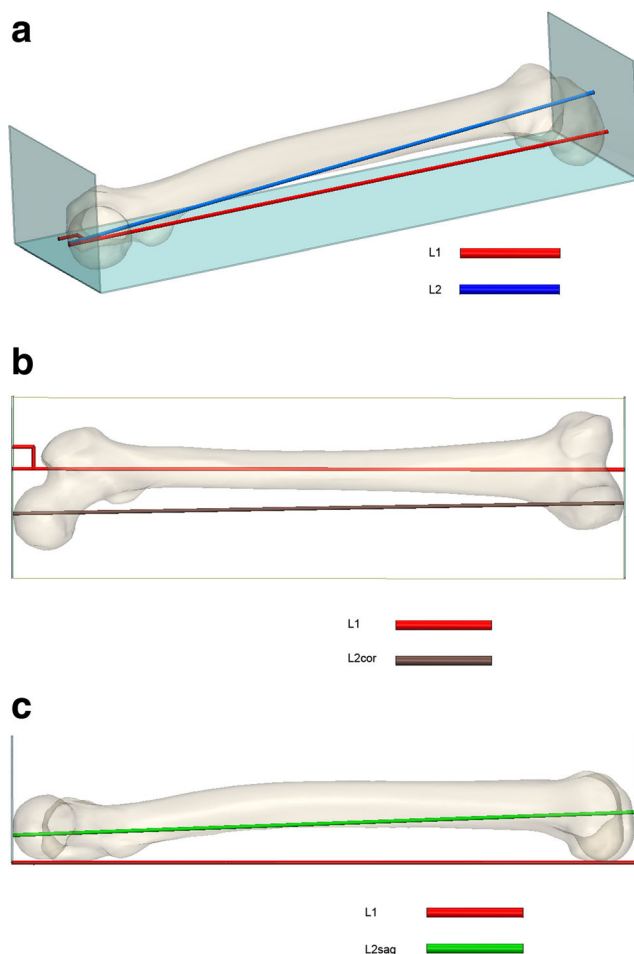


Fig. 1 Three-dimensional volume rendered visualization of a femur. The femur is put on the virtual osteometric board (a). The L1 (red) is the distance between two vertical (*axial*) planes which refers to the maximum femur length that is analogous to the classic method using osteometric board. The L2 (blue) is the line drawn between two contact points where each end of femur meets the two vertical planes. From the anterior view (b) of the femur, L2cor is the projection of the L2 to the horizontal (*coronal*) plane. From the lateral view (c) of the femur, L2sag is the projection of the L2 to the imaginary sagittal plane which is not shown in this figure

This study investigated how the CT images can be used for measurements in place of the osteometric board and how the stature estimation formula for Koreans is obtained.

Material and method

Subjects

A total of 390 Korean cadavers, including 30 skeletonized and 360 nonskeletonized ones, were subjected to the postmortem CT and autopsy at the National Forensic Service, Seoul Institute from September 2013 to February 2015. The data from the 30 skeletonized bones were used to compare the maximum femur lengths measured using an osteometric board with femur lengths measured using digitalized data. The data from the 52 cadavers out of 360 non-skeletonized ones were obtained using CAD data. The subjects in this group consisted of 15 females (the number of cadavers aged 10–20 = 4, aged 21–30 = 6, aged 31–40 = 4, and aged 41–50 = 1) and 37 males (the number of cadavers aged 10–20 = 5, aged 21–30 = 21, aged 31–40 = 10, and aged 41–50 = 1). The data from the remaining 308 non-skeletonized cadavers were collected to calculate stature estimation formulae for the modern Korean population. This group consisted of 153 females (the number of cadavers aged 10–20 = 6, aged 21–30 = 8, aged 31–40 = 33, aged 41–50 = 41, aged 51–60 = 28, aged 61–70 = 11, aged 71–80 = 19, and aged 81–90 = 7) and 155 males (the number of cadavers aged 10–20 = 2, aged 21–30 = 7, aged 31–40 = 17, aged 41–50 = 43, aged 51–60 = 59, aged 61–70 = 17, aged 71–80 = 7, and aged 81–90 = 3). All non-skeletonized cadavers with any abnormality such as fracture, deformity, or pathologic changes were excluded. The stature was measured in a supine position with a body ruler (Thermo Scientific, USA) at the beginning of the autopsy.

Procedures

A full body CT scan was performed with an MDCT (SOMATOM Definition As+, Siemens Healthcare, Erlangen, Germany) according to the National Forensic Service (NFS) protocol. This included a tube voltage of 120 kV, pitch factor of 0.35, slice thickness of 0.75 mm, increment of 0.7 mm, and rotation time of 0.3 s. Acquired images were used for measurement with image processing software (Aquarius iNtuition Edition version 4.4.7, TeraRecon Inc., CA, USA). The maximum femur length was measured using curved planar reformats (CPR) and rotating the image.

Data acquisition

DICOM files were converted to CAD data using the MIMICS software. After the segmentation process by the software, the femur was located on the imaginary horizontal (*coronal*) plane. This was confirmed by checking that the three lowest points of

the femur were on that plane. A center line in the shaft area was created automatically using the MIMICS software and then projected on the horizontal (coronal) plane. Two additional vertical (axial) planes were added that were perpendicular to the projected center line and also to the horizontal (coronal) plane. These two vertical (axial) planes are located at the most proximal point of the femur and at the most distal point of the femur by using the “Create Datum Plane” and “Create extreme analysis” function of the software. The distance between these vertical (axial) planes is the maximum femur length. This is the same method that is used when obtaining measurements with the osteometric board [20]. All the points, including landmarks on the surface of the femur have specific coordinates that make it possible to measure all the lengths.

To verify the reason why measurements in 3D are almost the same to ones measured by the classic method using the osteometric board, a line (L2 in Fig. 1a) was drawn between the two contact points on the two vertical (axial) planes and checked whether it was parallel to the projected center line (L1 in Fig. 1a) of the long axis of the femur shaft on the horizontal (coronal) plane. The angle (θ) between these two lines was calculated using an inner product space of the vectors as:

$$\text{Inner product} = \vec{L1} \cdot \vec{L2} = |\vec{L1}| |\vec{L2}| \cos\theta$$

$$\theta = \arccosine\left(\frac{\vec{L1} \cdot \vec{L2}}{|\vec{L1}| |\vec{L2}|}\right)$$

From the anterior view (Fig. 1b) of the femur, L2cor was obtained from the projection of the L2 to the horizontal (coronal) plane. The angle (θ_A) between L2cor and L1 was calculated using an inner product space of the vectors as:

$$\text{Inner product} = \vec{L1} \cdot \vec{L2cor} = |\vec{L1}| |\vec{L2cor}| \cos\theta_A$$

$$\theta_A = \arccosine\left(\frac{\vec{L1} \cdot \vec{L2cor}}{|\vec{L1}| |\vec{L2cor}|}\right)$$

The coordinates of the L2sag could not be obtained from the lateral view (Fig. 1c) of the femur, because the imaginary sagittal plane where the L2 would be projected was not established. Since the length of the L1 was already measured and the height could be calculated from the coordinates of the L2, the angle (θ_L) between L2sag and L1 was calculated using a tangent function instead of using an inner product space of the vector as:

$$\theta_L = \arctangent((z_p - z_d)/L1)$$

z_p : z value of the proximal end of L2
 z_d : z value of the distal end of L2

Statistical analysis

The statistical analysis was performed using the SPSS 17.0 (SPSS, Chicago, IL). A Bland-Altman analysis was

performed to evaluate the agreement between the digital image method and the classical anthropological method using the osteometric board [21]. Simple linear regression analysis was performed to obtain the stature estimation formula.

Results

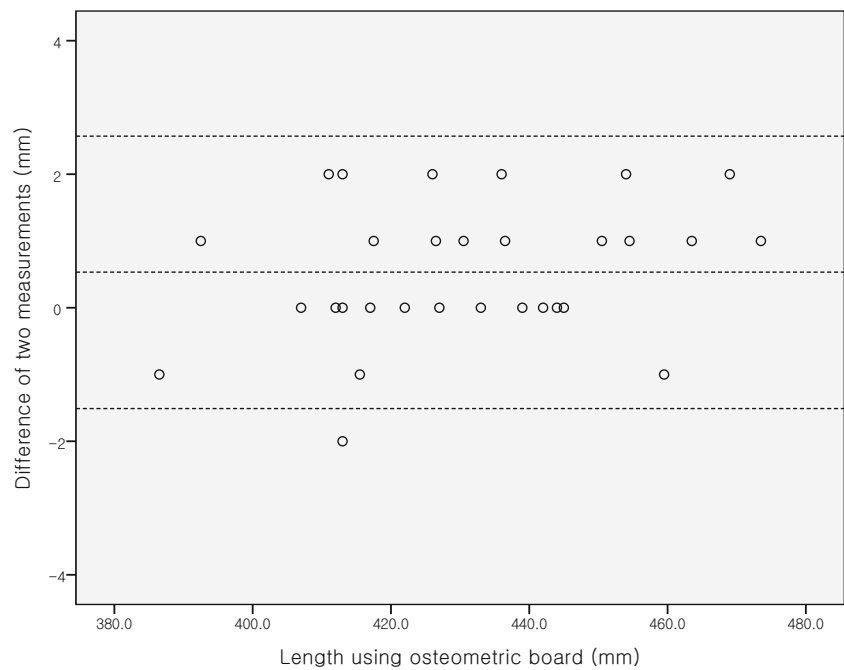
The measurements of 30 skeletonized femur specimens are listed in Table 1. After DNA analysis of bone fragments, the sexes were identified: 3 females and 27 males. The differences in osteological and CT measurements were plotted (Fig. 2). The average difference was 0.53 mm, and the maximum difference was 2 mm. Most of the measurements were in agreement with the Bland-Altman analysis.

Table 1 Measurements of skeletonized femur

No.	Side	Sex	L_{OB}	L_{CT}	$L_{OB}-L_{CT}$
1	R	M	422	422	0
2	L	M	427	425	2
3	R	F	407	407	0
4	L	M	427	427	0
5	R	M	437	435	2
6	L	M	442	442	0
7	L	F	386	387	-1
8	L	M	459	460	-1
9	R	M	439	439	0
10	R	M	455	454	1
11	L	M	455	453	2
12	L	M	427	426	1
13	R	M	444	444	0
14	R	M	393	392	1
15	R	M	412	412	0
16	L	M	415	416	-1
17	R	M	414	412	2
18	L	M	412	414	-2
19	L	M	412	410	2
20	R	F	413	413	0
21	L	M	474	473	1
22	R	M	417	417	0
23	L	M	418	417	1
24	R	M	470	468	2
25	L	M	433	433	0
26	R	M	445	445	0
27	L	M	464	463	1
28	R	M	451	450	1
29	R	M	431	430	1
30	L	M	437	436	1

R right, L left, M male, F female, L_{OB} measurements using osteometric board, L_{CT} measurements using digital data, all lengths are described in millimeter

Fig. 2 The result of the Bland-Altman analysis. All the differences between two measurements ($L_{OB}-L_{CT}$) are calculated to be below 2. L_{OB} is the femur length measured using osteometric board, and L_{CT} is the femur length measured using CT



The data of the 52 non-skeletonized subjects was converted to CAD data. The coordinates of the two contact points on the vertical (axial) planes and the two center line projected points of the long axis of the femur shaft on the horizontal (coronal) planes are listed in Table 2. The angles (θ) between the two lines (L1 and L2) obtained from each coordinate were calculated with an average of 1.48° and a maximum angle of 3.33° . The coordinates of the two projected points of L2 on the horizontal (coronal) plane are listed in Table 3, which is how L2cor was obtained. The angles (θ_A) between the two lines (L1 and L2cor) indicated an average of 0.80° with a maximum angle of 3.07° . The angles (θ_L) between L1 and L2sag (Fig 1c) were calculated using the tangent function. The mean of the angles was 0.98° with a maximum angle of 2.76° .

The descriptive statistics of femur measurements from the 308 non-skeletonized individuals are shown in Table 4. The female stature ranged from 140.0 to 185.0 cm. The average was 157.11 cm with a standard deviation of 7.46 cm. In males, the stature ranged from 153.5 to 186.6 cm. The average was 169.59 cm with a standard deviation of 6.25 cm. There was a positive correlation between femur lengths and stature that was statistically significant using the Pearson correlation coefficient. A summary of the regression results is shown in Table 5. The coefficient of determination (R^2) values was high in all groups and higher in females than in males. The standard error of the estimate was lower in males than in females.

Discussion

Forensic anthropology is widely used for the determination of sex, age, and stature when severely decomposed or

skeletonized bodies are found [4, 22]. Recently, due to the development of MDCT, forensic radiology can play a role in forensic anthropology [12, 13, 23, 24]. Digital data can generate 3D models that can be easily maintained using computation equipment. In addition, structural information about unidentified bodies can be preserved using a 3D bone structure storage system that is applied to the data set without using a lot of storage space. A critical problem in using radiologic tools in the anthropologic field, however, is the difficulty in defining landmarks on 3D images. Landmark location uncertainty could cause technical errors in the process.

A method to prevent locating false landmarks was employed in this study. This method involves measuring the maximum femur length between the most proximal and most distal points in 3D space by rotating the image on the long axis of the femur using the CPR in MIMICS. During rotation, the most proximal and distal points can be changed according to each plane, and after a complete rotation, the maximum femur length can be determined. The measurements obtained using this method were comparable to measurements obtained using an osteometric board in the 30 skeletonized femurs. As in previous studies [25], the average length of the left femur was slightly greater than the average length of the right femur. The differences, however, were not statistically significant.

Of late, CT is considered to be an accurate radiologic assessment for morphometry in contrast to plain radiography [9, 26]. In this study, the classical osteometric board was virtually simulated using CAD data and specialized software. After measuring the maximum femur length, the DICOM files were converted into CAD data using the MIMICS software. The femur was segmented and placed

Table 2 Measurements of skeletonized femur. The coordinates of the two contact points on the vertical (axial) planes and two projected points of the center line on the horizontal (coronal) planes

No	C1x	C1y	C1z	C2x	C2y	C2z	V1x	V1y	V1z	V2x	V2y	V2z
1	992.09	918.39	763.35	747.15	796.14	763.35	1070.1	989.85	791.66	671.12	785.99	793.37
2	536.29	843.32	330.75	525.93	603.36	330.75	512.07	937.02	360.54	496.67	536.57	356.31
3	1014.84	805.58	893.85	155.06	928.11	893.85	831.18	867.49	930.86	356.5	931.45	925.99
4	646.05	1013.62	428.08	638.93	711.3	428.08	614.51	1105.37	455.33	609.69	650.92	456.93
5	700.89	1122.53	810.73	711.46	837.95	810.73	659.5	1225	845.73	686.58	776.7	838.92
6	620.67	944.68	154.58	612.94	652.53	154.58	596.34	1028.3	192.04	581.89	603.6	187.11
7	609.7	936.19	153.25	589.69	634	153.25	590.6	1057.26	201.36	550.92	579.7	189.45
8	642.14	1027.12	532.61	631.15	701.25	532.61	615.83	1117.52	559.27	602.23	646.4	562.25
9	673.7	1011.03	406.06	642.28	707.76	406.06	652.38	1085.17	445.88	614.03	657.04	430.52
10	618.6	996.76	502.19	617.23	680.56	502.19	577.37	1082.74	529.56	590.95	625.57	546.81
11	658.18	675.5	250.89	693.02	944.07	250.89	669.19	606	281.48	722.44	990.51	278.38
12	614.85	962.25	522.61	607.28	659.31	522.61	588.68	1049.18	556.31	580.11	611.27	564.32
13	634.6	1008.52	429.74	618.99	687.36	429.74	613	1103.58	522.78	585.17	624.15	521.04
14	682.14	667.43	147.95	661.46	367.9	147.95	659.4	749.46	175.53	632.06	314.68	176.19
15	655.75	1007.83	586.28	652.22	699.62	586.28	628.02	1073.95	609.48	624.97	657.22	623.86
16	678.21	1054.38	534.68	672.18	722.83	534.68	649.15	1144.38	563.84	640.99	661.37	571.07
17	661.61	1041.69	616.36	657.93	711.76	616.36	636.11	1121.51	653.38	627.45	667.77	638.93
18	647.29	1049.23	445.27	668.61	731.15	445.27	605.97	1129.98	478.34	649.46	681.26	484.35
19	651.31	965.04	285.77	636.3	683.72	285.77	633.04	1047.17	319.63	601.5	631.07	307.09
20	624.39	972.57	230.16	598.28	642.36	230.16	602.6	1063.62	271.46	561.57	584.73	261.72
21	605.9	958.58	284.49	588.7	651.35	284.49	582.12	1050.95	331.44	550.11	587.33	309.11
22	652.35	1002.7	556.89	617.39	696.87	556.89	640.27	1088.03	597.3	578.41	639.29	581.36
23	646.2	996.69	434.21	633.32	688.03	434.21	603.97	1091.87	474.09	599.26	630.01	479.45
24	734.5	1010.5	593.54	727.4	747.48	593.54	702.32	1076.49	616.7	707.25	704.13	628.47
25	651.55	989.54	621.96	650.16	712.17	621.96	621.71	1081.44	658.81	627.21	652.41	664.82
26	1059.74	771.79	763.9	790.62	781.93	763.9	1143.81	798.15	791.58	736.77	804.5	795.22
27	648.52	1022.88	523.58	648.56	712.98	523.58	615.29	1122.62	563.38	624.85	656.23	563.19
28	1043.76	700.19	673.08	726.43	707.73	673.08	1140.87	726.49	700.38	664.59	732.67	706.01
29	638.95	993.98	260.48	621.81	684.16	260.48	629.22	1083.05	299.8	590.31	622.65	292.2
30	730.24	1165.94	885.36	753.49	874.67	885.36	688.48	1251.05	918.73	729.31	814.32	913.27
31	664.15	983.62	300.42	611.85	676.2	300.42	646.45	1089.88	326.57	572.64	616.55	325.59
32	653.71	963.22	214.07	634.85	683.67	214.07	636.03	1041.05	257.99	601.61	635.74	244.43
33	649.01	971.95	290.54	620.68	683.36	290.54	628.05	1071.51	322.47	584.25	625.65	315.76
34	674.81	991.54	133.96	669.26	714.73	133.96	662.84	1075.78	169.2	647.61	664.64	169.52
35	662.75	968.87	473.22	633.22	684.15	473.22	634.58	1066.07	504.29	601.4	630.15	501.61
36	634.49	977.57	266.76	614.25	670.85	266.76	604.58	1064.04	299.17	579.29	616.86	292.96
37	608.73	959.5	222.7	595.04	645.81	222.7	584.46	1053.69	263.26	563.99	581.1	251.64
38	664.34	986.25	234.98	660.72	707.98	234.98	642.58	1081.35	273.74	644.1	655.18	281.18
39	619.82	913.26	562.6	613.92	678.19	562.6	602.51	1002.4	598.01	580.66	621.39	599.13
40	640.69	947.09	85.84	610.28	646.05	85.84	618.87	1026.77	128.88	574.31	597.65	114.39
41	645.53	949.75	218.94	604.55	664.63	218.94	612.87	1030.79	248.56	570.57	609.4	239.79
42	644.86	990.96	481.98	632.16	700.17	481.98	622.52	1066.68	522.19	600.28	642.67	508.04
43	669.06	1014.1	533.48	658.88	733.57	533.48	653.86	1098.75	564.62	631.55	691.01	550.4
44	648.42	961.56	117.2	604.42	651.74	117.2	636.94	1045.07	152.18	567.25	599.85	143.61
45	670.03	1013.1	529.2	672.21	728.02	529.2	632.68	1091.55	560.74	658.71	683.47	566.92
46	617.16	960.08	249.66	595.74	660.53	249.66	596.7	1047.8	296.81	564.82	601.22	283.03
47	689.15	1103.54	813.09	698.68	799.03	813.09	652.69	1191	844	676.24	747.67	847.17
48	620.78	952.95	362.67	613.79	669.71	362.67	592.98	1047.07	392.43	588.36	615.13	400.15
49	632.47	976.97	406.86	628.41	688.03	406.86	612.66	1069.11	427.97	598.73	639.47	424.79
50	642.68	1020.18	670	639.38	719.26	670	613.2	1113.84	700.76	607.8	650.06	703.36
51	1052.5	731.42	730.33	763.68	759.04	730.33	1140.76	758.35	764.32	709.99	791.8	757.92
52	661.09	1024.86	583.41	652.38	705.14	583.41	623.31	1117.65	619.98	622.22	646.05	619.33

All values are rounded off to the second decimal points

C1x x-coordinate of proximal contact point of the projected center line of the femur shaft, *C1y* y-coordinate of proximal contact point of the projected center line of the femur shaft, *C1z* z-coordinate of proximal contact point of the projected center line of the femur shaft, *C2x* x-coordinate of distal contact point of the projected center line of the femur shaft, *C2y* y-coordinate of distal contact point of the projected center line of the femur shaft, *C2z* z-coordinate of distal contact point of the projected center line of the femur shaft, *V1x* x-coordinate of proximal contact point on the vertical plane, *V1y* y-coordinate of proximal contact point on the vertical plane, *V1z* z-coordinate of proximal contact point on the vertical plane, *V2x* x-coordinate of distal contact point on the vertical plane, *V2y* y-coordinate of distal contact point on the vertical plane, *V2z* z-coordinate of distal contact point on the vertical plane

Table 3 The coordinates of two projected points on the horizontal (coronal) plane of both contact points on vertical (axial) planes

No	H1x	H1y	H1z	H2x	H2y	H2z
1	1069.53	991.07	763.36	671.11	785.99	763.36
2	513.59	936.96	330.75	496.67	536.57	330.75
3	831.42	868.52	893.85	356.5	931.45	893.84
4	614.51	1105.37	428.08	609.69	650.92	428.08
5	659.5	1225.01	810.73	686.58	776.71	810.73
6	596.34	1028.31	154.58	580.4	603.61	154.58
7	590.4	1057.31	153.25	551.91	579.41	153.25
8	615.74	1117.9	532.61	603.84	646.11	532.61
9	652.38	1085.18	406.06	614.03	657.05	406.06
10	576.05	1082.78	502.19	590.97	625.53	502.19
11	669.71	605.81	250.89	722.44	990.65	250.89
12	589.79	1049.23	522.61	572.76	611.01	522.61
13	613	1103.58	492.74	585.17	624.16	492.74
14	658.9	749.5	147.95	632.06	314.68	147.95
15	625.55	1074.4	586.28	621.44	656.6	586.28
16	652.63	1144.37	534.68	637.11	661.41	534.68
17	631.79	1121.6	616.36	628.64	667.67	616.36
18	605.97	1129.98	445.27	649.46	681.26	445.27
19	627.55	1047.82	285.77	603.82	630.71	285.77
20	600.57	1063.8	230.16	561.57	584.72	230.16
21	580.29	1051.14	284.49	551.84	587.19	284.49
22	640.27	1088.03	556.89	578.42	638.3	556.89
23	604.81	1091.87	434.21	590.55	629.93	434.21
24	704.87	1076.48	593.54	705.77	704.11	593.54
25	625.86	1081.45	621.96	625.51	652.41	621.96
26	1143.85	798.97	763.9	736.77	804.5	763.9
27	615.29	1122.62	523.58	624.85	656.22	523.58
28	1140.87	726.49	673.08	664.59	732.67	673.08
29	627.81	1083.19	260.48	590.76	622.56	260.48
30	685.74	1250.87	885.36	729.31	814.33	885.36
31	644.15	1090.35	300.42	572.86	616.51	300.42
32	635.32	1041.14	214.07	601.71	635.42	214.07
33	625.91	1071.79	290.54	585.82	625.31	290.54
34	656.15	1076.16	133.96	643.53	664.05	133.96
35	634.58	1066.07	473.22	601.39	630.16	473.22
36	604.58	1064.04	266.76	579.29	616.86	266.76
37	579.36	1054.01	222.7	565.45	580.99	222.7
38	642.58	1081.36	234.98	636.4	655.22	234.98
39	602.51	1002.4	562.6	577.3	621.14	562.6
40	618.37	1026.83	85.84	574.46	597.47	85.84
41	610.47	1031.24	218.94	572.74	609.11	218.94
42	620.27	1066.89	481.98	601.87	642.45	481.98
43	648.83	1099.31	533.48	631.55	691.01	533.48
44	636.11	1045.33	117.2	568.19	599.54	117.2
45	640.43	1091.86	529.21	648.41	682.53	529.2
46	596.7	1047.79	249.66	565.1	601.11	249.66
47	652.69	1191	813.09	676.24	747.67	813.09
48	597.66	1047.1	362.67	584.52	615.1	362.67
49	612.42	1069.36	406.86	600.78	639.41	406.86
50	613.2	1113.84	670	610.16	649.97	670
51	1140.75	758.35	730.33	709.98	791.8	730.33
52	623.31	1117.65	583.41	621.93	645.97	583.41

All values are rounded off to the second decimal points

H1x x-coordinate of proximal contact point after projecting on the horizontal plane, *H1y* y-coordinate of proximal contact point after projecting on the horizontal plane, *H1z* z-coordinate of proximal contact point after projecting on the horizontal plane, *H2x* x-coordinate of distal contact point after projecting on the horizontal plane, *H2y* y-coordinate of distal contact point after projecting on the horizontal plane, *H2z* z-coordinate of distal contact point after projecting on the horizontal plane

on an imaginary horizontal plane. Two additional imaginary vertical planes were added, which were perpendicular to the horizontal plane. The maximum femur length was then calculated from the distance between the two

vertical planes. This is similar to the classic method using an osteometric board [20]. As in previous studies, the measurements using CT images were comparable to the measurements using an osteometric board [13, 27, 28].

Table 4 Descriptive statistics of measurements (cm) of femur

	Female (<i>n</i> = 153)				Male (<i>n</i> = 155)			
	Minimum	Maximum	Mean	S.D.	Minimum	Maximum	Mean	S.D.
Right	32.1	48.1	40.853	2.3548	38.8	50.6	44.123	2.0487
Left	32.2	47.9	40.935	2.3268	38.5	50.8	44.254	2.0566

S.D. standard deviation

CAD data was used to determine the reason that the measurements were similar. In Fig. 1, the maximum femur length measured using the osteometric board was designated L1, and the maximum length measured using CT was designated L2. The two lengths are the same when the two lines are parallel. When using CAD data, all the points on the surface of the femur have specific coordinates. Length can be easily calculated when any two contact points of any line is known. Maximum femur length can be calculated when the coordinates of two contact points on the femur and two imaginary vertical planes are known. To calculate the angle between any two lines, the inner product space of the vector can be used. The angle between L1 and L2 was almost zero in every measurement. This means that the line between the two contact points on the osteometric board was almost always parallel to the base planes and also to the long axis of the shaft of the femur.

The stature estimation formula for Korean adults was obtained using CT images. Simple linear regression analysis is an appropriate statistical method for stature estimation analysis [29, 30]. There has been a lack of research on a stature estimation formula for Asian females. Choi et al. used the long bones of Korean adults to present a stature estimation formula, but did not include females in the study [19]. Extremities of stature proportions are different compared to those in the past owing to different lifestyles. Therefore, new stature estimation formulae are needed to reflect modern relative leg length [3, 31]. There is a little difference between the formulae for stature estimation of Koreans and other populations. The regression coefficients

of the stature estimation formula in this study are higher than those in previous studies with other populations but lower than those in the study by Choi et al. [3, 19] of the Korean male population. They are also higher in the female population than in the male population. This study used cadaver lengths, which are known to be greater than living stature lengths [3, 32, 33]. Therefore, further study using the data of living person is needed.

Conclusion

When using the digital images for measurement of the long bones, the frequently overlooked problem is whether the maximum femur length measured using CT image was comparable to the maximum femur length measured using osteometric board. We designed a virtual osteometric board to confirm anatomical characteristics of the femur and were able to validate the possibility to use the digital image in forensic anthropology and obtain a stature estimation formula for Korean population. In addition, this technique is expected to be applied in further studies using the data of other bones or living person.

References

1. Zeybek G, Ergur I, Demiroglu Z (2008) Stature estimation using foot measurements. *Forensic Sci Int* 181:54.e1–54.e5. doi:10.1016/j.forsciint.2008.08.003
2. Duyar I, Pelin C (2003) Body height estimation based on tibia length in different stature groups. *Am J Phys Anthropol* 122:23–27
3. Hasegawa I, Uenishi K, Fukunaga T, Kimura R, Osawa M (2009) Stature estimation formula from radiographically determined limb bone length in a modern Japanese population. *Leg Med (Tokyo)* 11: 260–266
4. Scheuer L (2002) Application of osteology to forensic medicine. *Clin Anat* 15(4):297–312
5. Cordeiro C, Munoz-Barus JI, Wasterlain S, Cunha E, Vieira DN (2009) Predicting adult stature from metatarsal length in a Portuguese population. *Forensic Sci Int* 193(1–3):131.e1–131.e4
6. Krishan K (2008) Determination of stature from foot and its segments in a north Indian population. *AM J Forensic Med Pathol* 29(4):297–303

Table 5 Summary of the regression results

	Regression equation	<i>R</i>	<i>R</i> ²	SEE
Female, right	2.82*FL + 41.926	0.890	0.792	3.4167
Female, left	2.842*FL + 40.776	0.886	0.785	3.4684
Male, right	2.593*FL + 55.170	0.850	0.722	3.3053
Male, left	2.610*FL + 54.081	0.859	0.737	3.2139

Values are indicated in centimeters.

FL femur length, *R* coefficient of correlation, *R*² coefficient of determination, *SEE* standard error of the estimate

7. Ozaslan A, Iscan MY, Ozaslan I, Tugcu H, Koc S (2003) Estimation of stature from body parts. *Forensic Sci Int* 132(1):40–45
8. Torimitsu S, Makino Y, Saitoh H et al (2014) Stature estimation in Japanese cadavers using the sacral and coccygeal length measured with multidetector computed tomography. *Leg Med (Tokyo)* 16(1):14–19
9. Giurazza F, Del Vescovo R, Schena E et al (2013) Stature estimation from scapular measurements by CT scan evaluation in an Italian population. *Leg Med (Tokyo)* 15(4):202–208
10. Giurazza F, Del Vescovo R, Schena E et al (2012) Determination of stature from skeletal and skull measurements by CT scan evaluation. *Forensic Sci Int* 222(1–3):398.e1–398.e9
11. Robert IS, Benamore RE, Benbow EW et al (2012) Post-mortem imaging as an alternative to autopsy in the diagnosis of adult deaths: a validation study. *Lancet* 379(9811):136–142
12. Robinson C, Eisma R, Morgan B et al (2008) Anthropological measurement of lower limb and foot bones using multi-detector computed tomography. *J Forensic Sci* 53(6):1289–1295
13. Brough AL, Bennett J, Morgan B et al (2013) Anthropological measurement of the juvenile clavicle using multi-detector computed tomography—affirming reliability. *J Forensic Sci* 58(4):946–951
14. Harris EF, Smith RN (2009) Accounting for measurement error: a critical but often overlooked process. *Arch Oral Biol* 54(Suppl 1):S107–S117
15. Gaia BF, Pinheiro LR, Umetsubo OS (2014) Accuracy and reliability of linear measurements using 3-dimensional computed tomographic imaging software for Le Fort I Osteotomy. *Br J Oral Maxillofac Surg* 52(9):873
16. Mall G, Hubig M, Büttner A, Kuznik J, Penning R, Graw M (2001) Sex determination and estimation of stature from the long bones of the arm. *Forensic Sci Int* 117(1–2):23–30
17. Verhoff MA, Ramsthaler F, Krähahn J, Deml U, Gille RJ, Grabherr S, Thali MJ, Kreutz K (2008) Digital forensic osteology—possibilities in cooperation with the Virtopsy project. *Forensic Sci Int* 174:152–156
18. Petrovecki V, Mayer D, Slaus M, Strinović D, Skavić J (2007) Prediction of stature based on radiographic measurements of cadaver long bones: a study of the Croatian population. *J Forensic Sci* 52(3):547–552
19. Choi BY, Chae YM, Chung IH, Kang HS (1997) Correlation between the postmortem stature and the dried limb-bone lengths of Korean adult males. *Yonsei Med J* 38(2):79–85
20. Saukko P, Knight B (2013) *Knight’s forensic pathology*, 4th edn. CRC press, Boca Raton
21. Bland JM, Altman DG (1986) Statistical methods for assessing agreement between two methods of clinical measurement. *Lancet* 1(8476):307–310
22. Guyomarc’h P, Santos F, Dutailly B et al (2012) Three-dimensional computer-assisted craniometrics: a comparison of the uncertainty in measurement induced by surface reconstruction performed by two computer programs. *Forensic Sci Int* 219(1–3):221–227
23. O’Donnell C, Woodford N (2008) Post-mortem radiology—a new sub-specialty? *Clin Radiol* 63(11):1189–1194
24. Hishmat AM, Michiue T, Sogawa N et al (2015) Virtual CT morphometry of lower limb long bones for estimation of the sex using postmortem Japanese adult data in forensic identification. *Int J Legal Med* 129(5):1173–1182
25. Telkka A (1950) On the prediction of human stature from the long bones. *Acta Anat (Basel)* 9(1–2):103–117
26. Blane CE, Hezenberg JE, DiPietro MA (1991) Radiographic imaging for Ilizarov limb lengthening in children. *Pediatr Radiol* 21(2):117–120
27. Stull KE, Tise ML, Ali Z, Fowler DR (2014) Accuracy and reliability of measurements obtained from computed tomography 3D volume rendered images. *Forensic Sci Int* 238:133–140
28. Valeri CJ, Cole TM 3rd, Lele S, Richtsmeier JT (1998) Capturing data from three-dimensional surfaces using fuzzy landmarks. *Am J Phys Anthropol* 107:113–124
29. Byers S, Akoshima K, Curran B (1989) Determination of adult stature from metatarsal length. *Am J Phys Anthropol* 79(3):275–279
30. Rodriguez S, Conzalez A, Simon A et al (2014) The use of computerized tomography in determining stature and sex from metatarsal bones. *Leg Med (Tokyo)* 16(5):252–257
31. Ali MA, Uetake T, Ohtsuki F (2000) Secular changes in relative leg length in post-war Japan. *Am J Hum Biol* 12(3):405–416
32. Marinho L, Almeida D, Santos A (2012) Is the length of the sternum reliable for estimating adult stature? A pilot study using fresh sterna and a test of two methods using dry sterna. *Forensic Sci Int* 220(1–3):292.e1–292.e4
33. Hauser R, Smolinski J, Gos T (2005) The estimation of stature on the basis of measurements of the femur. *Forensic Sci Int* 147(2–3):185–190